Molecular Pain

MPX Express
Accepted on 2 August, 2017
This article can be cited as 10.1177/1744806917730254

Kindlin-1 is a key protein in hyperbaric oxygen therapy for the treatment of neuropathic pain

Baisong Zhao[1*], Erning He[2*], Yongying Pan[1], Haiping Xu[1], and Xingrong Song[1]

[1]Department of Anesthesiology, Guangzhou Women and Children's Medical Center, Guangzhou Medical University, Guangzhou 510623, China

[2]Department of Anesthesiology, Nanning Second People's Hospital, Guangxi Medical University, Nanning 530031, China

*Two authors contributed equally to the work.

Corresponding Author:

Xingrong Song, Department of Anesthesiology, Guangzhou Women and Children's Medical Center, No. 9 Jinsui Road, Tianhe District, Guangzhou, Guangdong 510623, China.

Email: songxingrong510623@163.com

Molecular Pain

MPX Express
Accepted on 2 August, 2017
This article can be cited as 10.1177/1744806917730254

Abstract

BACKGROUND: Hyperbaric oxygen (HBO) therapy is increasingly used in adjuvant therapies to treat neupropathic pain (NPP). However, the specific targets of HBO treatment in NPP remains unclear. Recently we found that HBO therapy produces an antinociceptive response via the kindlin-1/wnt-10a signaling pathway in a chronic pain injury model in rats.

METHODS: The rats received an intraperitoneal injection of AAV-FERMT1 or an AAV control vector 20 days before the chronic constriction injury (CCI) operation. During five consecutive days of HBO treatment, mechanical withdrawal threshold (MWT) and thermal withdrawal latency (TWL) tests were performed. Then, kindlin-1 expression was examined by Real-time PCR and Western blot analysis. Meanwhile, the activation of glial cells and the production of TNF-α, IL-1β, and fractalkine were also determined.

RESULTS: Our findings demonstrated that HBO therapy inhibited the CCI-induced increase in kindlin-1 expression. Furthermore, over-expression of kindlin-1 reversed the antinociceptive effects of HBO therapy. The observed HBO-induced reductions in glial cell activation and neuroinflammation, as indicated by the production of TNF-α, IL-1β, and fractalkine, were also prominently diminished in the group with kindlin-1 over-expression.

MPX Express
Accepted on 2 August, 2017
This article can be cited as 10.1177/1744806917730254

CONCLUSIONS: Our findings demonstrate that kindlin-1 is a key protein in the action of HBO therapy in the treatment of NPP. Indeed, interference with kindlin-1 may be a drug target for reducing the neuroinflammatory responses of the glial population in NPP.

Keywords

kindlin-1; hyperbaric oxygen; neuropathic pain; chronic constriction injury; glial activation.

Molecular Pain

MPX Express
Accepted on 2 August, 2017
This article can be cited as 10.1177/1744806917730254

Introduction

Neuropathic pain (NPP), characterized by allodynia, hyperalgesia, spontaneous pain, and paraesthesia[1], is one of the most intense types of chronic pain. Several systemic retrospective studies have shown that patients with neuropathic pain report a lower quality of life than those with other chronic diseases such as cancer, diabetes, chronic heart failure, and stroke[2, 3]. Neuropathic pain is often difficult to control because of its complex etiology, including infectious agents, metabolic disease, neurodegenerative disease, and physical trauma[4-6]. Considering that present drug therapies are insufficient to meet the clinical demand of patients[7, 8], the development of new treatment options for this disease is likely to emerge from an in-depth understanding of its underlying etiological mechanisms.

Nonpharmacological approaches in the treatment of neuropathic pain have been shown to significantly alleviate neuropathic pain[9-11]. These approaches, such as transcutaneous electrical nerve stimulation, transcranial magnetic stimulation, acupuncture, ultrasound, regular exercise, and hyperbaric oxygen (HBO), are increasingly used as adjuvant therapies to treat pathological pain[12, 13] . In rats with chronic constriction injury (CCI), we found that HBO treatment produced a long-lasting antinociceptive effect[14]. Furthermore, different HBO treatment programs employed different mechanisms to inhibit nociception at different stages following CCI: early HBO treatment was associated with the inhibition of P2X4R expression, while late HBO treatment resulted in the inhibition of cell apoptosis[15]. A related study

MPX Express
Accepted on 2 August, 2017
This article can be cited as 10.1177/1744806917730254

also indicated that HBO therapy alleviated CCI-induced neuropathic pain and inhibited the production of tumor necrosis factor-α[16]. However, the specific target of HBO therapy for the treatment of neuropathic pain remains unclear.

Recently we reported, for the first time, that HBO treatment attenuated CCI-induced neuropathic pain via regulating the kindlin-1/Wnt-10a signaling pathway[17]. However, whether or not HBO therapy improves neuropathic pain via a mechanism which is dependent on kindlin-1 has not been definitively established. In the study reported herein, we sought to determine if over-expression of kindlin-1 influences the neurologic outcome and inflammation after HBO treatment in CCI-induced neuropathic pain.

Materials and methods

Animals

This study was conducted in strict accordance with the recommendations outlined in the Chinese Guide for the Care and Use of Laboratory Animals of the National Institutes of Health, and under approved protocols of the Institutional Animal Ethics Committee of the Guangzhou Medical University (2016-016). The protocol was approved by the Institutional Animal Ethics Committee of Guangzhou Medical University. All surgery was performed under sodium pentobarbital anesthesia and all efforts were made to minimize animal suffering. Forty-eight adult male Sprague-Dawley rats (8 – 10 weeks old, weighing 250 – 280 g) were used in this study. The animals were housed individually in plastic boxes under ambient temperature

MPX Express
Accepted on 2 August, 2017
This article can be cited as 10.1177/1744806917730254

conditions of 23 – 25 ºC with standard chow and water available *ad libitum*. These rats were randomly assigned to six groups (n = 8 for each group): the Sham group, CCI group, HBO (HBO treatment began one day postoperatively and was applied daily for five days after CCI) group, K1 group (intraperitoneal injection of AAV-9 vector 20 days prior to the sham operation), K2 group (intraperitoneal injection of AAV-9 vector 20 days prior to CCI), and the K3 group (intraperitoneal injection of AAV-9 vector 20 days prior to the CCI operation followed by HBO treatment beginning one day postoperatively and with application daily for five days after CCI).

Induction of neuropathic pain

The CCI model of the sciatic nerve was used to create neuropathic pain as described previously[18]. Briefly, rats were anesthetized by intraperitoneal injection of sodium pentobarbital (40 mg/kg). The left biceps femoris of each rat was bluntly dissected at the mid-thigh level to expose the sciatic nerve. Four 4-0 chromic catgut sutures were loosely tied around the sciatic nerve at 1 mm intervals immediately proximal to the trifurcation. The wound was then sutured in layers. For the sham group, an identical dissection was performed, but the sciatic nerve was not ligated.

Hyperbaric oxygen treatment

The cylindrical HBO treatment chamber (DS400-IV, Weifang Huaxin Oxygen Industry Co., Ltd., Shandong, China) was pre-coated with soda lime on the bottom to minimize water vapor and CO_2 accumulation. The chamber was ventilated with 100%

MPX Express
Accepted on 2 August, 2017
This article can be cited as 10.1177/1744806917730254

oxygen for 10 min as described previously[19]. After a rat was placed in the chamber, the pressure was increased at a rate of 0.1 ATA/min to the desired pressure (2.0 ATA) and maintained for 60 min. The rats were allowed to breathe spontaneously during the HBO treatment. The chamber was then decompressed to normal room pressure at a rate of 0.1 ATA/min. For rats in the HBO and K3 groups, HBO treatment began on postoperative day one and was carried out once a day for five consecutive days. Rats in the sham and CCI groups were placed inside the chamber without HBO treatment.

AAV vector construction and production.

The plasmids used in this study are shown in Fig. 1. To construct kindlin-1 (encoded by the *FERMT1* gene) expression vector, the rat *FERMT1* coding sequence (NM_001106515) was amplified with primers: *FERMT1*f, 5'-CGCAAATGGGCGGTAGGCGTG-3', and *FERMT1*r, 5'-CATAGCGTAAAAGGAGCAACA-3', and linked to the 3' end of the CMV promoter from the pAAV-CMV-MCS vector with interchanging recombination. The construct was confirmed via PCR and sequencing. The Adeno-associated virus (AAV) vectors were produced using a three-plasmid expression system. Briefly, human 293T cells were transfected with an AAV vector (expressing the *FERMT1*), an AAV helper plasmid (pAAV Helper), and an AAV Rep/Cap expression plasmid. Then, 72 h after transfection, the cells were collected and lysed using a freeze-thaw procedure. Viral particles were purified by an iodixanol step-gradient

MPX Express
Accepted on 2 August, 2017
This article can be cited as 10.1177/1744806917730254

ultracentrifugation method. The iodixanol was diluted, and the AAV was concentrated using a 100 kDa molecular mass cut-off ultrafiltration device [20]. The genomic titer was 1.89×10^{13} infectious unit per mL, determined by quantitative PCR. Systemic AAV9 gene transfer by intraperitoneal injection showed their distribution in the spinal cord and the dorsal root ganglia.

Behavioral tests

Mechanical withdrawal threshold (MWT) and thermal withdrawal latency (TWL) tests were performed on preoperative day 1 and postoperative days 1, 2, 3, 4, 5, 6, and 7. Each animal was placed in a Plexiglas chamber and habituated for 1 h prior to each test session before and after HBO treatment.

The MWT test was carried out to assess the response of the paw to a mechanical stimulus. The rats were placed in a Plexiglas chamber, and the MWT test was performed by stimulating the plantar surface of the left hind paw using von Frey filaments (Stoelting Company, USA). Each von Frey filament was held for approximately 3 – 5 seconds. Each trial started with the application of a 0.6 – 15.0 g von Frey force following the up-and-down procedure. A positive response was defined as a quick withdrawal of the hind paw upon stimulation. The cut-off value was 15 g. The paw threshold test was performed ten times, and the paw withdrawal threshold was defined as the von Frey force that caused 50% withdrawal.

To examine TWL, a BME-410C full-automatic plantar analgesia tester (Youer

MPX Express
Accepted on 2 August, 2017
This article can be cited as 10.1177/1744806917730254

Equipment Scientific Co., Ltd., Shanghai, China) was used to measure the sensitivity of the paw to thermal stimuli. The thermal withdrawal latency test was performed by placing the rats on the surface of a 3 mm thick glass plate that was covered with the same Plexiglas chamber. The radiant heat source was positioned at a fixed distance below the glass plate. Heat stimuli were directed at the exposure site on the left hind paw. The TWL was defined as the elapsed time (in seconds) to withdraw the paw from the heat source. Each test session included the delivery of five thermal stimuli at 5 min intervals and the mean latency is reported. A cut-off time of 30 seconds was set to avoid tissue damage.

Tissue Preparation

After completion of the behavioral tests on postoperative day 7, the rats (n = 8 per group) were anesthetized by intraperitoneal injection of sodium pentobarbital (40 mg/kg). Four rats in each group were transcardially perfused with 200 mL of normal saline. The spinal cord of each rat, between the L4 and L6 segments, was carefully removed and used for immunohistochemistry. Tissues from the other four animals were stored at -80 °C and used for Western blotting, Real-time, and enzyme-linked immunosorbent assay (ELISA).

Western blotting

The spinal cord tissues were homogenized on ice in lysis buffer. Protein concentrations were determined through the bicinchoninic acid assay method. The

MPX Express
Accepted on 2 August, 2017
This article can be cited as 10.1177/1744806917730254

proteins were resolved by sodium dodecyl sulfate–polyacrylamide gel electrophoresis and transferred onto polyvinylidene fluoride membranes by electroblotting. The membranes were incubated with primary antibodies against kindlin-1 (dilution 1:1000, ABCOM, USA) at 4 °C overnight. β-actin was used as a loading control. The membranes were then incubated with alkaline phosphatase-linked mouse anti-rabbit secondary antibodies (dilution 1:2000, Santa Cruz Biotechnology, USA) at room temperature for 2 h. The bands were visualized using a chemiluminescence detection system and analyzed with ScionImage software. The expression of kindlin-1 was normalized to that of β-actin.

Real-time PCR

Total spinal cord RNA was isolated according to the manufacturer's instructions using a Trizol kit (Life Technologies). RNA samples were then standardized and reverse transcribed with a Transcriptor First Strand cDNA Synthesis kit (Roche), according to the manufacturer's instructions using an oligo-dT/random nonamer primer mix. Quantitative real-time PCR (qRT-PCR) was carried out using the Roche FS Universal SYBR Green Master (Roche) system according to the manufacturer's instructions and a Viia7 system from Applied Biosystems. The primer sequences for kindlin-1 were 5'- GAGGCAGGGAAAACGACTGA -3' and 5'- CAGCCTGCTAGGTCTTGCTT -3'. Thermal cycling parameters started with 10 min at 95 °C, followed by 40 cycles of 95 °C for 15 seconds, 60 °C for 30 seconds and 72 °C for 30 seconds. Specificity of the PCR products was verified by melting curve

MPX Express
Accepted on 2 August, 2017
This article can be cited as 10.1177/1744806917730254

analysis.

Immunohistochemistry

The tissues were post-fixed and dehydrated in 30% sucrose in PBS at 4 °C for 24 hours and frozen sections were prepared. The spinal cord tissue sections (10 μm thick) were incubated at 4 °C overnight with a mouse anti-rat primary antibody against GFAP (1:200 dilution, ab7260; Abcam, USA) or a rabbit anti-rat primary antibody against Iba1 (1:200 dilution, ab5076; Abcam, USA), followed by incubation with biotinylated donkey anti-mouse or anti-rabbit IgG antibodies (1:200 dilution; Vector Laboratories, Burlingame, CA) in 1.5% normal donkey serum (NDS; Jackson Immuno Research Laboratories Inc., West Grove, PA) for 20 min at 37 °C. All sections were cover-slipped with a mixture of 50% glycerin in 0.01 mol/L PBS and then observed under a Leica SP2 confocal laser scanning microscope (Leica, Wetzlar, Germany). The mean intensity of immunoreactive staining for GFAP or Iba1 was measured with the Image J analysis system (National Institutes of Health, Bethesda, MD, USA). For each animal, eight sections of spinal L4 – 6 were randomly selected for quantitative evaluation. The corrected density values of the eight sections were averaged to provide a mean density for each animal. All behavioral testing and the quantification of immunohistochemical experiments were performed blind with respect to treatment.

Examination of TNF-α, IL-1β, and fractalkine production

MPX Express
Accepted on 2 August, 2017
This article can be cited as 10.1177/1744806917730254

The levels of TNF-α, IL-1β, and fractalkine in the spinal cord were measured by the ELISA (Wuhan Boster Biological Technology Co., Ltd., Wuhan, China)[21]. The unilateral spinal cord was dissected, ground with a grinder, and loaded onto an ultrasonic tissue homogenizer. The supernatant was collected after centrifugation. The production levels of TNF-α, IL-1β, and IL-10 were evaluated using ELISA kits according to the manufacturer's instructions. The optical density values at 490 nm were recorded using a microplate reader (NK3; Ladsystems, Helsinki, Finland). The average levels of TNF-α, IL-1β, and IL-10 were calculated based on the standard curve.

Statistical analysis

Analyses were performed using SPSS 17.0 (SPSS Inc., Chicago, IL, USA). Numerical data with normal distribution are presented as mean and standard deviation. Data without normal distribution are presented as median and percentiles. One way analysis of variance (ANOVA) was used to compare differences among groups. MWT and TWL were analyzed by one-way ANOVA followed by Scheffé and Dunnett tests. The recovery time of the hind limb movement was analyzed by the Kruskal-Wallis test followed by the Mann-Whitney U-test. Statistical significance was considered as $P < 0.05$.

Results

Kindlin-1 expression was elevated in the spinal cords of rats with CCI-induced NPP,

MPX Express
Accepted on 2 August, 2017
This article can be cited as 10.1177/1744806917730254

which was inhibited by HBO therapy

Firstly, we examined the effects of HBO treatment on the expression of kindlin-1 in the rat spinal cord. As shown in Fig. 2A and 2B, the protein expression of kindlin-1 was clearly elevated in the rat spinal cords of the CCI group seven days postoperative, and was depressed in those belonging to the HBO group after continuous five day HBO therapy. As shown in Fig. 2C the alteration of kindlin-1 mRNA expression was consistent with its protein levels. Thus, these results indicate that continuous HBO therapy can effectively inhibit the CCI-induced upregulation of kindlin-1.

Over-expression of kindlin-1 can reverse the curative effects of HBO therapy in the treatment of NPP

We then assessed if kindlin-1 had an influence on the effects of HBO-NPP therapy by introducing kindlin-1 over-expression in the rat spinal cord. Interestingly, we found that over-expression of kindlin-1 significantly decreased the paw withdrawal threshold (Fig. 3A) and the thermal pain threshold (Fig. 3B) 4 to 7 days postoperatively, indicating that over-expression of kindlin-1 can reverse the curative effects of HBO therapy on NPP, as shown in the K3 group. Moreover, there were no significant differences between the sham group and K1 group or between the CCI group and K2 group, indicating that the over-expression of kindlin-1 did not affect the basic threshold and the postoperative threshold of CCI. Thus, it can be concluded that over-expression of kindlin-1 only affected the analgesic effect of HBO therapy.

Over-expression of kindlin-1 can block the anti-inflammatory effects of HBO therapy

MPX Express
Accepted on 2 August, 2017
This article can be cited as 10.1177/1744806917730254

Next, we addressed the effects of kindlin-1 over-expression on the production of TNF-α, IL-1β, and fractalkine in the spinal cord (Fig. 4). Compared with the CCI group, the concentrations of TNF-α (A), IL-1β (B), and fractalkine (C) were significantly lower in the rat spinal cord of the HBO group, which indicates that HBO therapy had anti-inflammatory effects. However, with over-expression of kindlin-1 in the spinal cord of group K3 rats subjected to the same HBO therapy, the levels of TNF-α, IL-1β, and fractalkine increased. This indicates over-expression of kindlin-1 can block the anti-inflammatory role of HBO therapy. It is worth noting that over-expression of kindlin-1 only affected the anti-inflammatory responses to HBO therapy, not the production of inflammatory cytokines under basal conditions and after CCI.

Over-expression of kindlin-1 expression can block the action of HBO therapy in inhibiting the activation of glial cells

To assess CCI-induced glia activation, we analyzed the expression levels of Iba1 (a microglial-specific antibody marker) and GFAP (a suitable marker of astrocytes) in rats. The results show that while HBO therapy can effectively inhibit the expression of Iba1 (Fig. 5) and GFAP (Fig. 6) in the spinal cord of CCI rats, the over-expression of kindlin-1 diminishes the effects of HBO therapy on inhibiting glia activation. Moreover, a comparison of the activation of rat spinal microglial cells and astrocytes found that over-expression of kindlin-1 had no effect on the ratio of activated microglial cells to astrocytes in the rat spinal cord.

MPX Express
Accepted on 2 August, 2017
This article can be cited as 10.1177/1744806917730254

Discussion

The major finding of this study is that over-expression of kindlin-1 can diminish the antinociceptive effect of HBO therapy on neurologic outcome, inflammation, and glial cell activation. These data represent the first definitive evidence that kindlin-1 contributes to the mechanism that underpins the actions of HBO treatment on neuropathic pain, at least in part by initiating inflammation and glial cell activation. Nerve injury can activate astrocytes and microglia[21], which synthesize and secrete cytokines, inflammatory mediators, and neural active substances[22, 23]. Excessive accumulation of these substances sensitize these glial cells, thus contributing to the development and sustenance of NPP[24]. Previous studies reported by our group indicate that HBO treatment has obvious therapeutic effects in the treatment of NPP[14, 15]. Furthermore, consecutive hyperbaric oxygen treatments could obviously inhibit the activated microglia and astrocytes in the dorsal horn of spinal cord in rats with NPP, as reported in the present study.

There is a considerable amount of evidence that shows that the activity of cell adhesion molecules (CAM) is closely related to glial cell activation and cell infiltration in an abnormal response of the central nervous system [25-28]. As a small team of members in the big CAM family, integrins are a set of transmembrane receptors that directly connect to the extracellular matrix (ECM) and facilitate communication between intracellular signaling pathways by regulating integrin ligands[29-31]. As previously reported[32, 33], excessive expression of the kindlin family,

MPX Express
Accepted on 2 August, 2017
This article can be cited as 10.1177/1744806917730254

such as kindlin-1 and kindlin-2, will lead to excessive activation of integrins or inflammation and tumor cell infiltration. However, blocking or competitively inhibiting the combination of kindlin and talin proteins with integrins could effectively block the activation of integrins[34] and inflammation processes[35]. We previously reported that HBO treatment attenuated CCI-induced neuropathic pain via regulating the kindlin-1/Wnt-10a signaling pathway [17]. In the present study, we further discovered that over-expression of kindlin-1 could diminish the protective effect of HBO treatment. These results indicate that kindlin-1 may be a key target protein in HBO therapy for NPP. Interestingly, we also found a difference in variation between mechanical hypersensitivity and thermal hypersensitivity. There are two possible reasons for this phenomenon and its occurrence. One is that, under the CCI model, mechanical hypersensitivity is more sensitive than thermal hypersensitivity to facilitate better discrimination. Another reason is that over-expression of kindlin-1 is more likely to lead to the occurrence of mechanical hyperalgesia. The specific mechanism needs to be confirmed by further experiments.

Interestingly, though excessive expression or kindlin-1 led to excessive activation of integrins, inflammation, and tumor cell infiltration, over-expression of kindlin-1 did not affect the pain behavior and biochemical indicators of rats. These results suggest that the regulatory role of kindlin-1 on NPP may be secondary to nerve injury. Thus, it can be surmised that while kindlin-1 is a key target protein in HBO therapy for NPP, it is not key in the pathophysiological process of NPP.

MPX Express
Accepted on 2 August, 2017
This article can be cited as 10.1177/1744806917730254

In summary, we found that hyperbaric oxygen could inhibit the activation of glial cells and reduced the production of inflammatory cytokines via inhibiting the expression of kindlin-1 in the treatment of neuropathic pain. This information provides a new theoretical basis for hyperbaric oxygen treatment of neuropathic pain. Interference with kindlin-1 may prove to be a drug target for reducing neuroinflammatory responses of glial cells in the pathogenesis of neuropathic pain.

Authors' contributions

BSZ carried out the molecular genetic studies, participated in the sequence alignment and drafted the manuscript. HPX carried out the behavioral, PCR and immunohistochemical analysis. YYP participated in the design of the study and performed the statistical analysis. XRS conceived the study, and participated in its design. ENH participated coordination and helped to draft the manuscript. All authors read and approved the final manuscript.

Declaration of conflicting interests

The author(s) declared no potential conflicts of interest with respect to the research, authorship, and/or publication of this article.

MPX Express
Accepted on 2 August, 2017
This article can be cited as 10.1177/1744806917730254

Funding

The author(s) disclosed receipt of the following financial support for the research, authorship, and/or publication of this article: This project was supported by the Guangzhou Institute of Pediatrics/Guangzhou Women and Children's Medical Center (grant no. YIP-2016-006).

References

1. Costigan M, Scholz J and Woolf CJ. Neuropathic pain: a maladaptive response of the nervous system to damage. *Annu Rev Neurosci*. 2009; 32: 1-32.
2. Doth AH, Hansson PT, Jensen MP and Taylor RS. The burden of neuropathic pain: a systematic review and meta-analysis of health utilities. *Pain*. 2010; 149: 338-44.
3. Smith BH, Torrance N, Bennett MI and Lee AJ. Health and quality of life associated with chronic pain of predominantly neuropathic origin in the community. *Clin J Pain*. 2007; 23: 143-9.
4. Almeida C, DeMaman A, Kusuda R, et al. Exercise therapy normalizes BDNF upregulation and glial hyperactivity in a mouse model of neuropathic pain. *Pain*. 2015; 156: 504-13.
5. Jain KK. Current challenges and future prospects in management of neuropathic pain. *Expert Rev Neurother*. 2008; 8: 1743-56.
6. Truini A, Garcia-Larrea L and Cruccu G. Reappraising neuropathic pain in humans--how symptoms help disclose mechanisms. *Nat Rev Neurol*. 2013; 9: 572-82.
7. Ledda F, Paratcha G, Sandoval-Guzman T and Ibanez CF. GDNF and GFRalpha1 promote formation of neuronal synapses by ligand-induced cell adhesion. *Nat Neurosci*. 2007; 10: 293-300.
8. Gilron I, Jensen TS and Dickenson AH. Combination pharmacotherapy for management of chronic pain: from bench to bedside. *Lancet Neurol*. 2013; 12: 1084-95.
9. Chatzitheodorou D, Kabitsis C, Malliou P and Mougios V. A pilot study of the effects of high-intensity aerobic exercise versus passive interventions on pain, disability, psychological strain, and serum cortisol concentrations in people with chronic low back pain. *Phys Ther*. 2007; 87: 304-12.
10. Hayden JA, van Tulder MW and Tomlinson G. Systematic review: strategies for using exercise therapy to improve outcomes in chronic low back pain. *Ann Intern Med*. 2005; 142: 776-85.

MPX Express
Accepted on 2 August, 2017
This article can be cited as 10.1177/1744806917730254

11. Norrbrink C, Lindberg T, Wahman K and Bjerkefors A. Effects of an exercise programme on musculoskeletal and neuropathic pain after spinal cord injury--results from a seated double-poling ergometer study. *Spinal Cord*. 2012; 50: 457-61.
12. Gu N, Niu JY, Liu WT, et al. Hyperbaric oxygen therapy attenuates neuropathic hyperalgesia in rats and idiopathic trigeminal neuralgia in patients. *Eur J Pain*. 2012; 16: 1094-105.
13. Nizard J, Lefaucheur JP, Helbert M, de Chauvigny E and Nguyen JP. Non-invasive stimulation therapies for the treatment of refractory pain. *Discov Med*. 2012; 14: 21-31.
14. Zhao BS, Meng LX, Ding YY and Cao YY. Hyperbaric oxygen treatment produces an antinociceptive response phase and inhibits astrocyte activation and inflammatory response in a rat model of neuropathic pain. *J Mol Neurosci*. 2014; 53: 251-61.
15. Zhao BS, Song XR, Hu PY, et al. Hyperbaric oxygen treatment at various stages following chronic constriction injury produces different antinociceptive effects via regulation of P2X4R expression and apoptosis. *PLoS One*. 2015; 10: e0120122.
16. Li F, Fang L, Huang S, et al. Hyperbaric oxygenation therapy alleviates chronic constrictive injury-induced neuropathic pain and reduces tumor necrosis factor-alpha production. *Anesth Analg*. 2011; 113: 626-33.
17. Zhao B, Pan Y, Xu H and Song X. Hyperbaric oxygen attenuates neuropathic pain and reverses inflammatory signaling likely via the Kindlin-1/Wnt-10a signaling pathway in the chronic pain injury model in rats. *J Headache Pain*. 2017; 18: 1.
18. Zhao B, Pan Y, Wang Z, Tan Y and Song X. Intrathecal Administration of Tempol Reduces Chronic Constriction Injury-Induced Neuropathic Pain in Rats by Increasing SOD Activity and Inhibiting NGF Expression. *Cell Mol Neurobiol*. 2016; 36: 893-906.
19. Zhao B, Pan Y, Wang Z, Xu H and Song X. Hyperbaric Oxygen Pretreatment Improves Cognition and Reduces Hippocampal Damage Via p38 Mitogen-Activated Protein Kinase in a Rat Model. *Yonsei Med J*. 2017; 58: 131-8.
20. Cheng TL, Wang Z, Liao Q, et al. MeCP2 suppresses nuclear microRNA processing and dendritic growth by regulating the DGCR8/Drosha complex. *Dev Cell*. 2014; 28: 547-60.
21. Milligan ED and Watkins LR. Pathological and protective roles of glia in chronic pain. *Nat Rev Neurosci*. 2009; 10: 23-36.
22. Tsuda M, Masuda T, Tozaki-Saitoh H and Inoue K. Microglial regulation of neuropathic pain. *J Pharmacol Sci*. 2013; 121: 89-94.
23. Zhuo M, Wu G and Wu U. Neuronal and microgiial mechanisms of neuropathic pain. *Mol Brain*. 2011; 4: 31.
24. Cao H and Zhang YQ. Spinal glial activation contributes to pathological pain states. *Neurosci Biobehav Rev*. 2008; 32: 972-83.
25. Corty MM and Freeman MR. Cell biology in neuroscience: Architects in neural circuit design: glia control neuron numbers and connectivity. *J Cell Biol*. 2013; 203: 395-405.
26. Engelhardt B. Immune cell entry into the central nervous system: involvement of adhesion molecules and chemokines. *J Neurol Sci*. 2008; 274: 23-6.

MPX Express
Accepted on 2 August, 2017
This article can be cited as 10.1177/1744806917730254

27. Hermosilla T, Munoz D, Herrera-Molina R, et al. Direct Thy-1/alphaVbeta3 integrin interaction mediates neuron to astrocyte communication. *Biochim Biophys Acta*. 2008; 1783: 1111-20.
28. Togashi H, Sakisaka T and Takai Y. Cell adhesion molecules in the central nervous system. *Cell Adh Migr*. 2009; 3: 29-35.
29. Kim SH, Turnbull J and Guimond S. Extracellular matrix and cell signalling: the dynamic cooperation of integrin, proteoglycan and growth factor receptor. *J Endocrinol*. 2011; 209: 139-51.
30. Myers JP, Santiago-Medina M and Gomez TM. Regulation of axonal outgrowth and pathfinding by integrin-ECM interactions. *Dev Neurobiol*. 2011; 71: 901-23.
31. Rout UK. Roles of Integrins and Intracellular Molecules in the Migration and Neuritogenesis of Fetal Cortical Neurons: MEK Regulates Only the Neuritogenesis. *Neurosci J*. 2013; 2013: 859257.
32. Shen Z, Ye Y, Kauttu T, et al. The novel focal adhesion gene kindlin-2 promotes the invasion of gastric cancer cells mediated by tumor-associated macrophages. *Oncol Rep*. 2013; 29: 791-7.
33. Ye F, Kim C and Ginsberg MH. Reconstruction of integrin activation. *Blood*. 2012; 119: 26-33.
34. Lu L, Zhang YH, Lin CD and Chen JF. Mechanisms Underlying Integrin Deactivation. *Chin J Cell Biol*. 2015; 37: 1-8.
35. Park EJ, Yuki Y, Kiyono H and Shimaoka M. Structural basis of blocking integrin activation and deactivation for anti-inflammation. *J Biomed Sci*. 2015; 22: 51.

MPX Express
Accepted on 2 August, 2017
This article can be cited as 10.1177/1744806917730254

Fig. 1. Diagram of plasmid structure. A refers to the profile of the blank-vector plasmid before the insertion of the target gene (Fermt1); B refers to the profile of the full-vector plasmid after the insertion of the target gene (Fermt1).

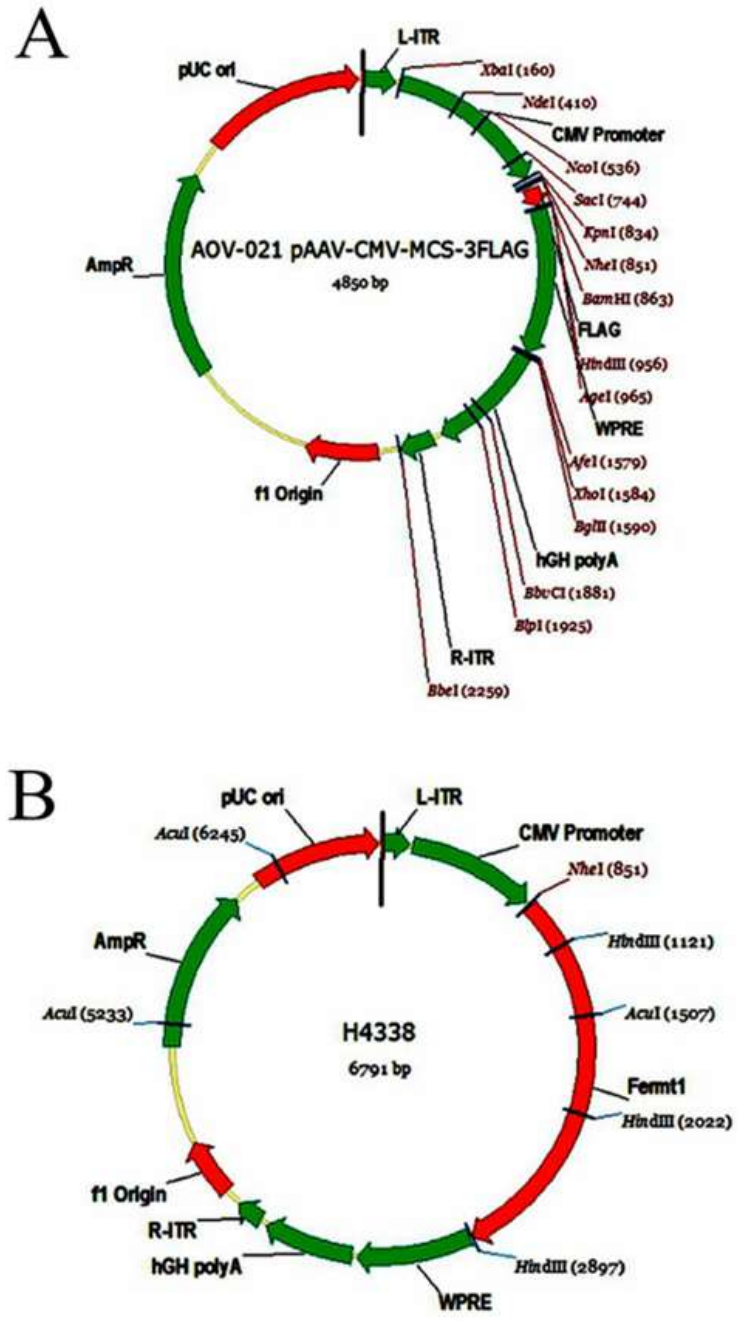

Molecular Pain

MPX Express
Accepted on 2 August, 2017
This article can be cited as 10.1177/1744806917730254

Fig. 2. Effect of HBO treatment on the expression of kindlin-1 in the spinal cord in rats in the Sham, CCI, and HBO groups 7 days postoperative. (A) Representative western blot results showing the expression of kindlin-1 in the spinal cord of rats in the Sham, CCI, and HBO groups. (B) The relative expression of kindlin-1 was normalized to the expression of β-actin. (C) RT-PCR results showing the expression of kindlin-1 in the Sham, CCI, and HBO groups *p < 0.05, ns p > 0.05 . n=4.

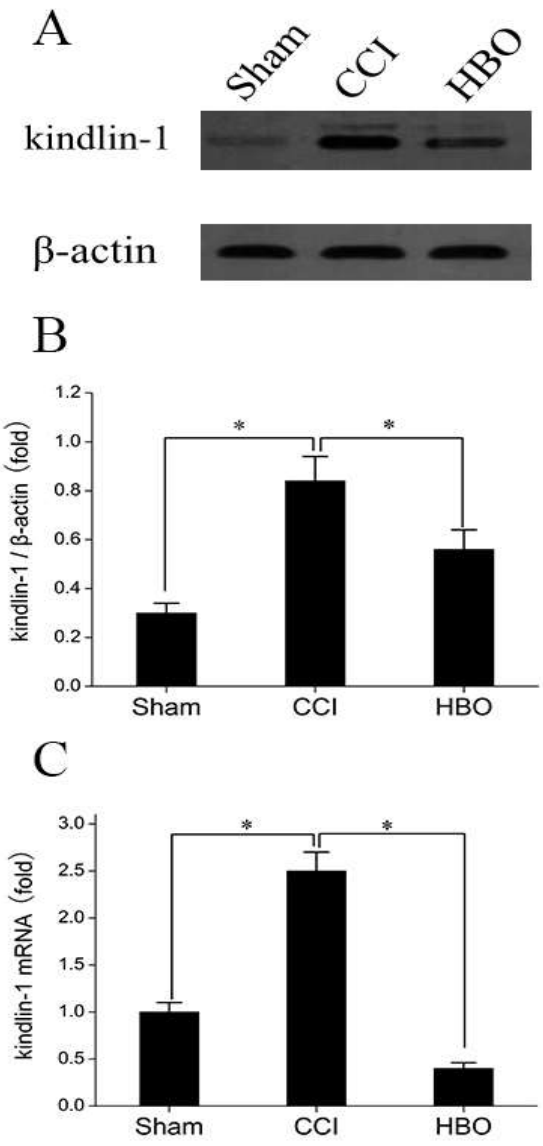

MPX Express
Accepted on 2 August, 2017
This article can be cited as 10.1177/1744806917730254

Fig. 3. The effect of HBO treatment on the MWT (A) and the TWL (B) in rats in the Sham, CCI, HBO, K1, K2, and K3 groups. MWT and TWL tests were performed on preoperative day 1 and postoperative days 1, 2, 3, 4, 5, 6, and 7. Compared with the Sham group, MWT and TWL were lower in the CCI, K2, and K3 groups resulting in apparent hyperalgesia. Compared with the CCI group, MWT and TWL were elevated in the HBO group, suggesting HBO therapy can inhibit hyperalgesia. Compared with the HBO group, MWT and TWL were lower in the K3 group, showing that even though the K3 group was also subjected to HBO therapy, over-expression of kindlin-1 can reverse the treatment role of HBO on NPP. *$p < 0.05$ vs. Sham, #$p < 0.05$ vs. CCI, &$p < 0.05$ vs. HBO. n=8.

Molecular Pain

MPX Express
Accepted on 2 August, 2017
This article can be cited as 10.1177/1744806917730254

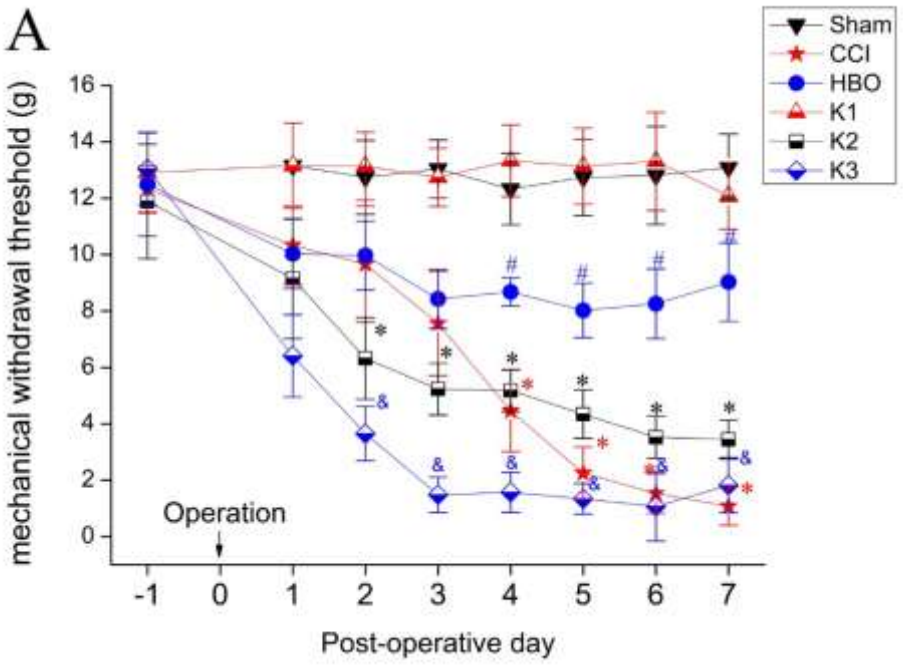

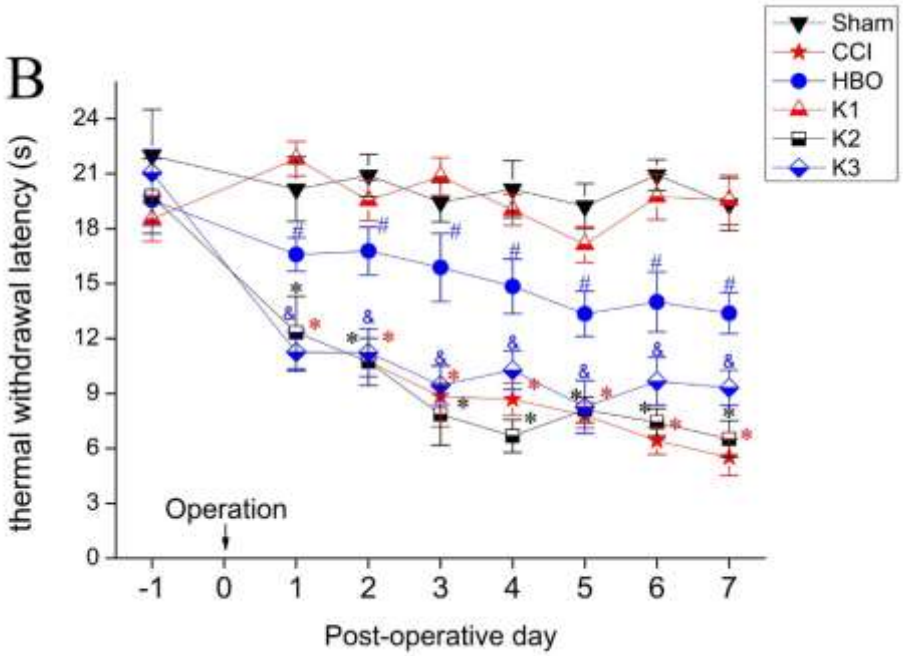

MPX Express
Accepted on 2 August, 2017
This article can be cited as 10.1177/1744806917730254

Fig. 4. Changes of TNF-α, IL-1β, and fractalkine levels in the rat spinal cords of each group 7 days postoperative. Compared with the CCI group, TNF-α, IL-1β, and fractalkine levels were lower in the HBO group, suggesting that HBO therapy can inhibit the inflammation of NNP in the rat spinal cord. Compared with the HBO group, TNF-α, IL-1β, and fractalkine levels were higher in the K3 group, suggesting that although the K3 group was subjected to the same HBO therapy, over-expression of kindlin-1 can reverse the anti-inflammatory role of HBO therapy. *$p < 0.05$, ns $p > 0.05$. n=4.

Molecular Pain

MPX Express
Accepted on 2 August, 2017
This article can be cited as 10.1177/1744806917730254

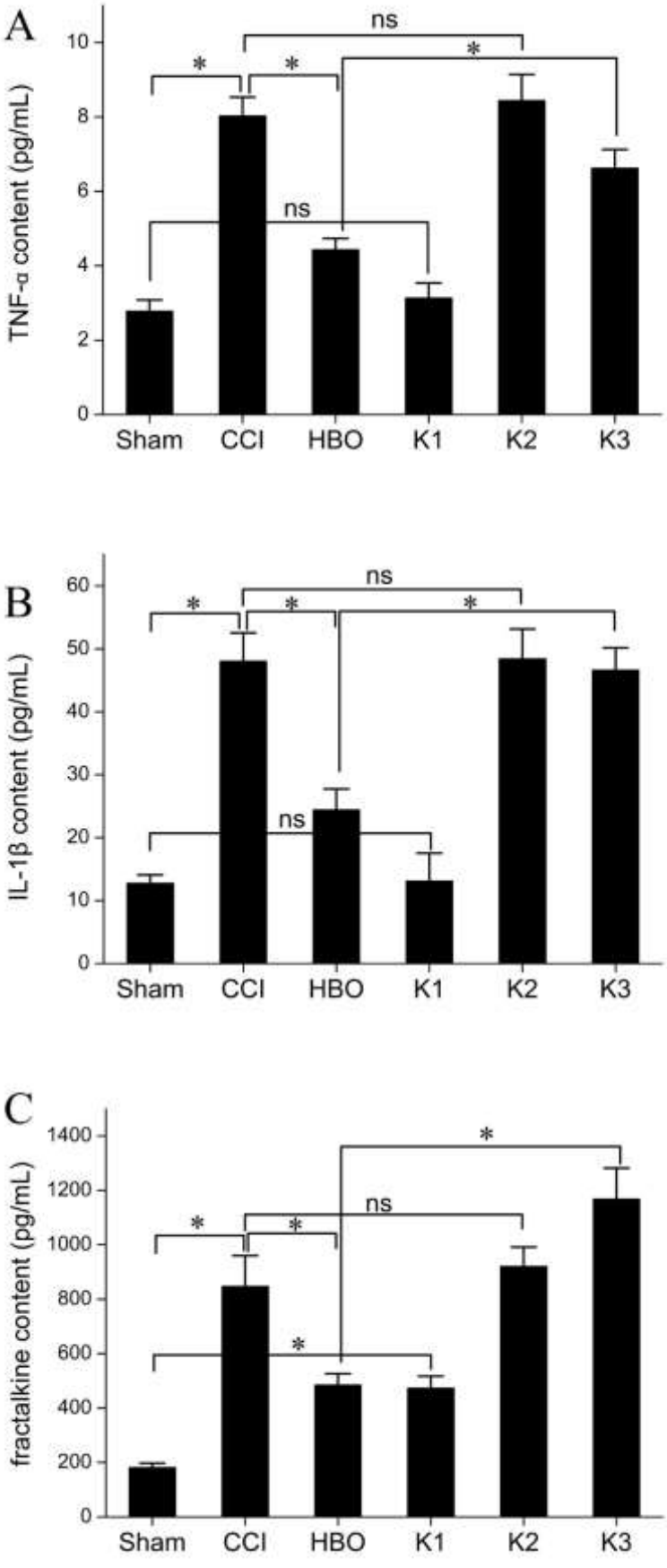

MPX Express
Accepted on 2 August, 2017
This article can be cited as 10.1177/1744806917730254

Fig. 5. Photomicrographs (A) and bar graph (B) showing microgila responses in the spinal dorsal horn 7 days postoperative. Little Iba1 immunostaining was observed in the Sham group, but the CCI group showed markedly increased Iba1 immunostaining. Iba1-immunostaining microgila profiles were characterized by big, thick, and irregular shaped cytoplasmic and spine ramified processes in the CCI group, and significantly fewer Iba1-immunoreactive microgilas were present in the HBO group than in the CCI group. Higher quantities of Iba1-immunoreactive microgilas were observed in the K3 group than in the HBO group. *$p < 0.05$, ns $p > 0.05$. n=4.

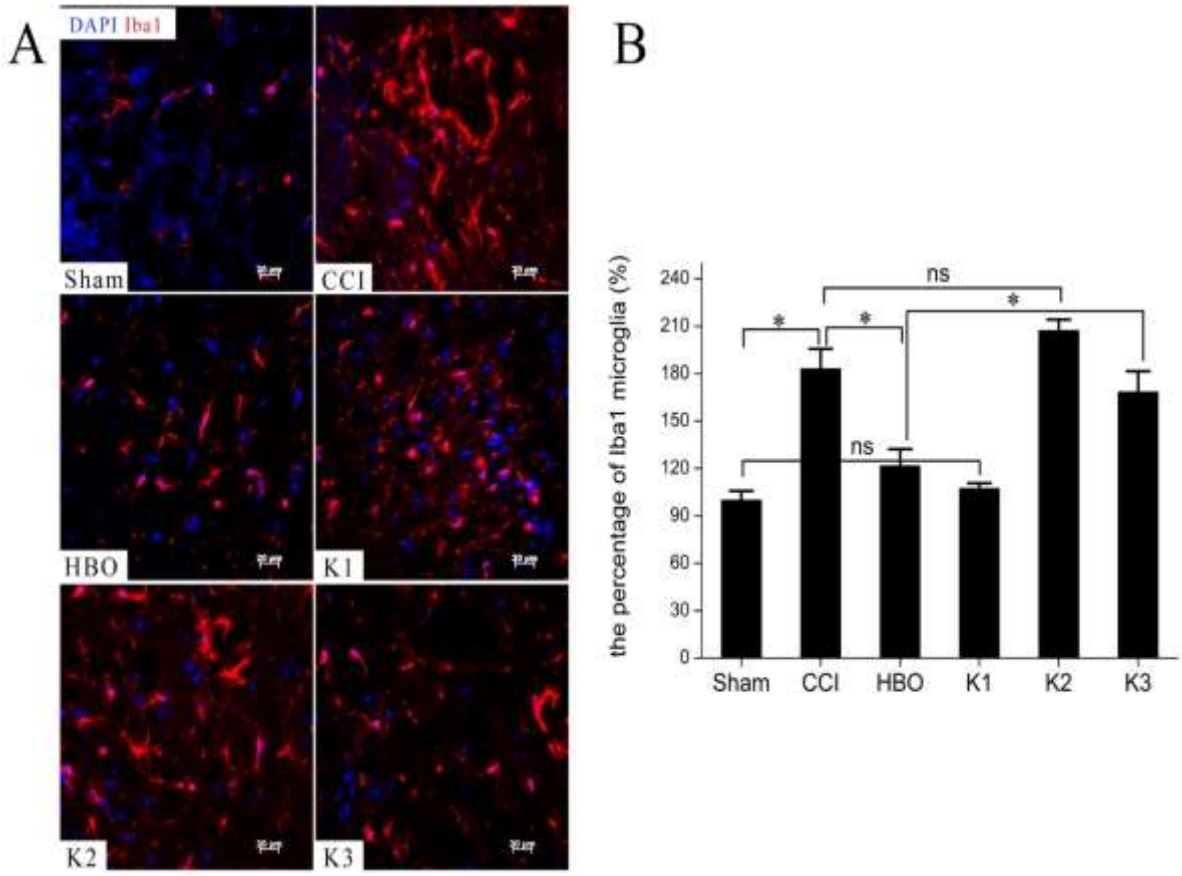

Molecular Pain

MPX Express
Accepted on 2 August, 2017
This article can be cited as 10.1177/1744806917730254

Fig. 6. Photomicrographs (A) and bar graph (B) showing astrocytic responses in the spinal dorsal horn 7 days postoperative. Little glial fibrillary acidic protein (GFAP) immunoreactivity was observed in the Sham group, but the CCI group showed markedly increased GFAP immunostaining. GFAP-immunostaining astrocytic profiles were characterized by small, compact cell bodies with long, thin ramified processes 7 days after HBO treatment, and significantly fewer GFAP-immunoreactive astrocytes were present in the HBO group than in the CCI group. Fewer GFAP-immunoreactive astrocytes were observed in the HBO group than in the K group. *p < 0.05, ns p > 0.05. n=4.